DOI https: //doi. org/10.1007/s11595-020-2312-7

# Calibration of Binding Energy Positions with C1s for XPS Results

**FANG De[1,2], HE Feng[1,3], XIE Junlin[1,2,3*], XUE Lihui[2]**

*(1. State Key Laboratory of Silicate Materials for Architectures, Wuhan University of Technology, Wuhan 430070, China; 2. Center for Materials Research and Analysis, Wuhan University of Technology, Wuhan 430070, China; 3. School of Materials Science and Engineering, Wuhan University of Technology, Wuhan 430070, China)*

**Abstract:** The adventitious carbon located at 284.8 eV was used to calibrate samples without the carbon themselves. When the carbon is as a major part of the inorganic material, the adventitious carbon should be identified and used as the reference. There is no adventitious carbon on the surfaces of the polymer materials, so using C1s of the carbon in the polymer itself to calibrate the charging effect is reasonable. Furthermore, compared with gold and argon, a more practical and convenient method based on C1s is proposed to get the right positions for binding energy peaks.

**Key words:** XPS; calibration; charging effect; binding energy; C1s

## 1 Introduction

As a surface analysis technique, X-ray photoelectron spectroscopy(XPS) has been widely used in the scientific researches[1-5], while the most notable of many features for XPS is the surface sensitivity[6-8]. The chemical states and quantitative information for most elements can be identified according to the position and intensity of the XPS peaks. Binding energy databases, such as the NIST database[9] or the Handbooks from Perkin-Elmer and Springer Co[10-12], can provide sufficient information to analyze the XPS data from the experiments. During the XPS tests, samples may be insulators, semiconductors or conductors from all walks of life. As shown in Fig.1, the charging effect takes place for insulators and semiconductors due to the escape of photoelectrons, but the conductors can obtain lots of electrons from the earth to avoid the charging effect. The charging effect can result in the stable surface potential that decreases the kinetic energy of photoelectrons, while the surface potential is related to

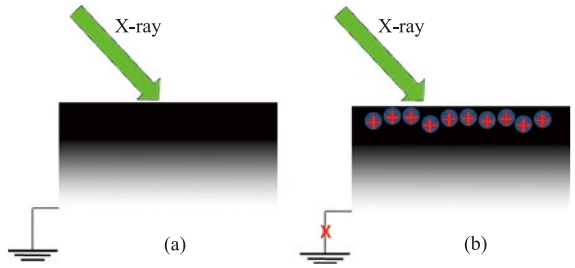


Fig.1 The charging effect during the XPS tests: (a) Conductors; (b) Insulators and semiconductors

the conducting properties, thickness, surface roughness and X-ray source. Meanwhile, the charging effect leads to the increasing of the binding energy and the changing (widening or distortion) of the curves, having a detrimental effect on the analysis of results[13-18]. Therefore, effective measures should be carried out in practical work to solve the energy deviation caused by the charging effect when the identification of chemical states is based on measurements of chemical shifts with accuracies in the range down to 0.1 eV[19]. In our practical work, the sample stage of the X-ray photoelectron spectroscopy measurement (ESCALAB 250Xi) is without earthing, since it is hard for the testers to evaluate the conducting properties of complex samples. All samples are regarded as non-conducting and they are posted on the insulation tape, while the flood gun is used to improve the charging effect by using the charging compensation. The right and frequently-used method is to compensate low energy electrons, but it is difficult to achieve prospective and



(Received: Sept. 16, 2019; Accepted: Nov. 7, 2019)

FANG De(方德): Assoc. Prof.; Ph D; E-mail: fangde0914@whut.edu.cn

*Corresponding author: XIE Junlin(谢峻林): Prof.; Ph D; E-mail: xjlclxy@126.com

Funded by the National Key R&D Program of China (2017YFC0210802) and the Fundamental Research Funds for the Central Universities (WUT: 2019III015GX)

accurate charge balance. Superfluous electrons are distributed on the surface of the sample in most cases, causing the peaks move the higher binding energy[20]. Meanwhile, the binding energy peaks can be removed to the right positions by subtracting about 2 eV according to our testing experiences.

The technique for charge referencing is needed, and some common methods are conductor, gold, adventitious carbon, internal hydrogen, co-condensed hydrocarbon, argon, valence band minimum and pure element[9]. There are three usual kinds of external standard materials considered as reference peak, such as carbon, argon and gold[17,21-24]. According to the binding energies of the adsorbed or deposited elements on the surfaces of samples, the binding energies of the other elements could be obtained. Argon possesses excellent chemical durability, so it is used as the reference when the surface cleaning process or depth analysis is performed with argon ions. The method is convenient and the measurement accuracy is about 0.3 eV[22], but the method cannot be used without the argon ion gun. Gold as the reference material (paints, pens or powders) can be put onto the samples[25], and the measurement accuracy is less than 0.2 eV[26]. The monolayer deposited gold should get electrical equilibrium with the sample and the measurement accuracy is related to the cover degree of the gold on the sample, which is difficult to control. Therefore, deposited gold as a reference is not widely deployed due to the complex operations. In most cases, the C1s line of adventitious hydrocarbon on air-exposed samples is used as the reference to calibrate XPS, and it is assumed to have a binding energy of 284.8 eV[9].

In this paper, the methods of calibrating the binding energy peak positions with C1s are discussed for the complex samples containing carbon (such as potassium carbonate, titanium carbide, nylon 66, polyethylene terephthalate and so on) or without carbon (such as tungsten trioxide, $Sr_{1-y}Eu_ySi_2O_{2-y}N_{2+2y/3}$ and so on) themselves when the flood gun is used during the XPS test. Based on the obtained results, in-depth understanding and analyzing of charging effects in these kinds of samples are illustrated, suggesting the normal way to get the right positions for binding energy peaks.

## 2 Experimental

All XPS tests are carried out on the ESCALAB 250Xi spectrometer (Thermo Fisher, USA). The background pressure of the analysis chamber is lower than $5\times10^{-10}$ mbar and that of the sample chamber is lower than $2\times10^{-8}$ mbar in standby mode. The background pressure of the analysis chamber is about $4\times10^{-8}$ mbar at working conditions when the flood gun was used to ameliorate the charging effect. “Charge Comp Standard” was selected as the beam mode when the samples are non-magnetic, and “Charge Comp Electrostatic” was appropriate for the magnetic samples. The spot of X-ray is mono 500 μm and the selected anode is aluminium, while the monitored values are about 14.2 kV and 11.3 mA. Meanwhile, XPS test parameters for survey and narrow scans are shown in the Table 1. Normally, the dispersion of the radiation source does allow keeping one decimal place. In this paper, two decimal places are kept to calibrate the charging effect, illustrating the whole calibration process.

**Table 1 XPS test parameters for survey and narrow scans**

| Test parameters | Survey scan | Narrow scan |
|---|---|---|
| Energy scale | Binding | Binding |
| Pass energy/eV | 100 | 30 |
| Number of scans | 1 | 5 |
| Dwell time/ms | 100 | 50 |
| Lens mode | Standard | Standard |
| Energy step size/eV | 1 | 0.1 |

## 3 Results and discussion

### 3.1 Sole adventitious carbon on the surface

It is difficult to avoid the adventitious carbon contamination for most samples unless the samples are prepared in the reaction chamber that is equipped on the conventional XPS equipment. However, it is worth noting that the researchers can take advantage of the C1s for calibrating spectra for a large proportion of materials, while there is only adventitious carbon in the sample. The binding energy of the C1s spectra of the adventitious carbon is generally believed to be at 284.80 eV.

Pure $WO_3$ was selected as the sample without containing carbon itself to analyze and calibrate the charging effect. Figs.2(a) and 2(c) are C1s and W4f spectra without calibrating, while Figs.2(b) and 2(d) are C1s and W4f spectra with calibrating. C1s in Fig.4(a) is 283.71 eV (without calibrating), so the shift is 1.09 eV that is used for calibrating W4f. $W4f_{7/2}$ is at 35.83 eV characterizing the $W^{6+}$ state in $WO_3$, which is in agreement with the previous researches[27-29]. Therefore,

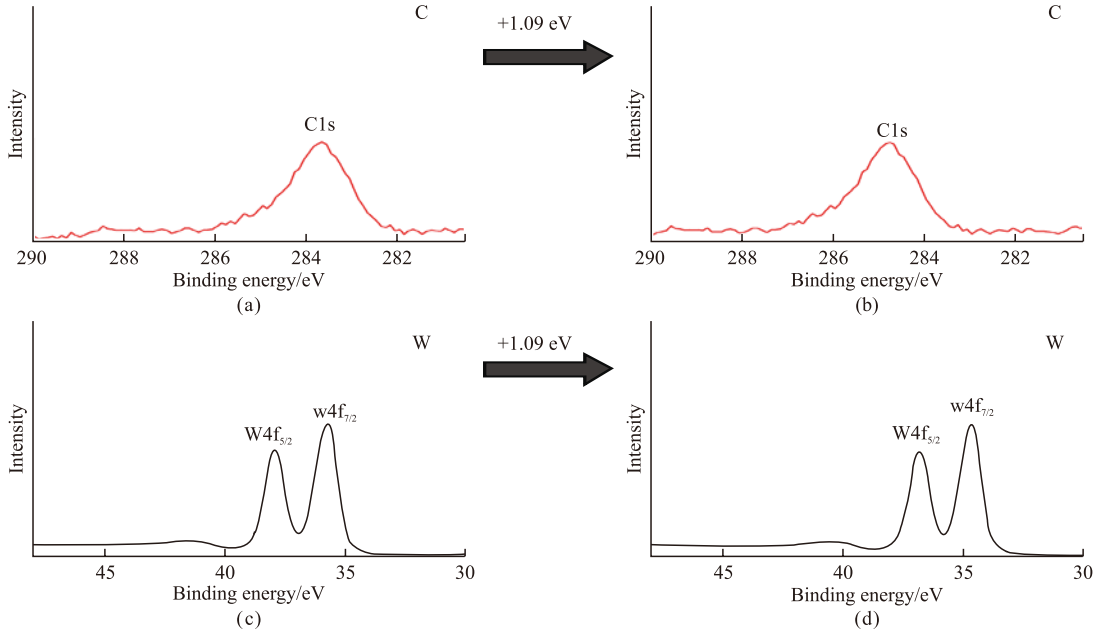


Fig.2 The C1s of adventitious carbon using as a reference for $WO_3$

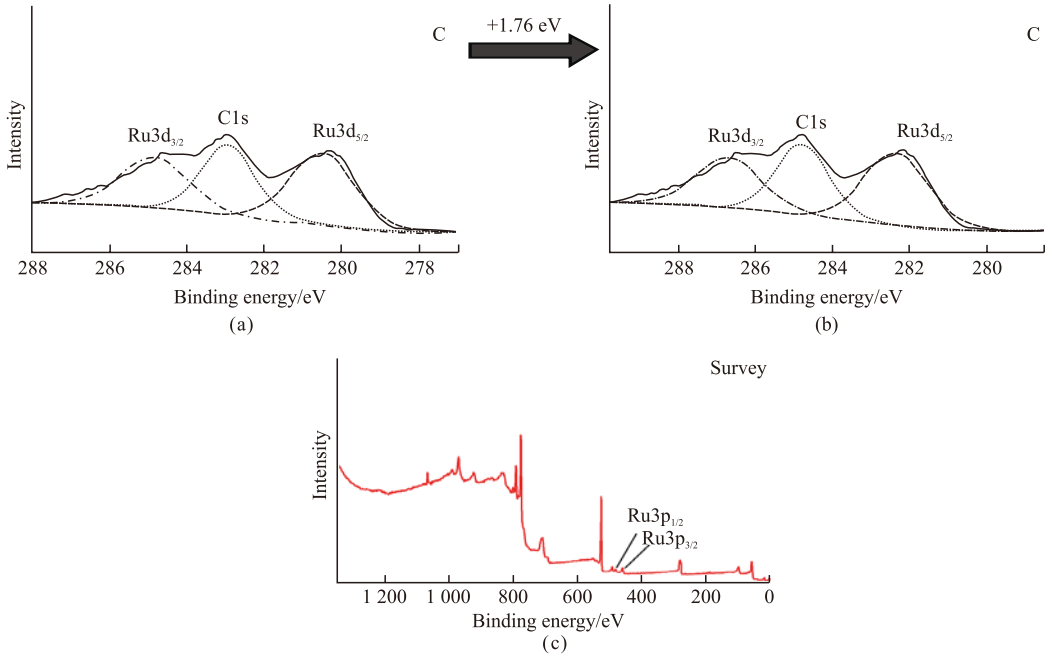


Fig.3 C1s and survey spectra of the mixture (cobalt hydroxide and ruthenium oxide)

using the C1s spectra of the adventitious carbon in the sample can be a viable and scientific option for calibrating the charging effect. However, there are some interference peaks during the analyzing the XPS data to calibrate the charging effect. Full dissociation should be made between the interference peaks and C1s peak.

As shown in Fig.3, a very strong overlap between the C1s peak and Ru3d peak (confirming by the survey in Fig.3(c)) takes place, so it is necessary to separate the two kinds of peak when the C1s peak of the adventitious carbon is used for calibrating the charging effect. A clean standard ruthenium material is selected to develop the fitting methodology with $Ru3d_{3/2}$ and $Ru3d_{5/2}$ peaks, and the C1s peak at 283.04 eV (without calibrating) is also required to obtain smaller residual error considering the presence of the adventitious carbon. Therefore, the shift is 1.76 eV that is used for calibrating other elements such as Ru and O.

As shown in the Fig.4, there are two peaks in the binding energy area of C1s, so it is worth noting that the two peaks should be identified. According to the survey, Eu exits in the fluorescent material ($Sr_{1-y}Eu_ySi_2O_{2-z}N_{2+2z/3}$) on account of the obvious $Eu3d_{3/2}$

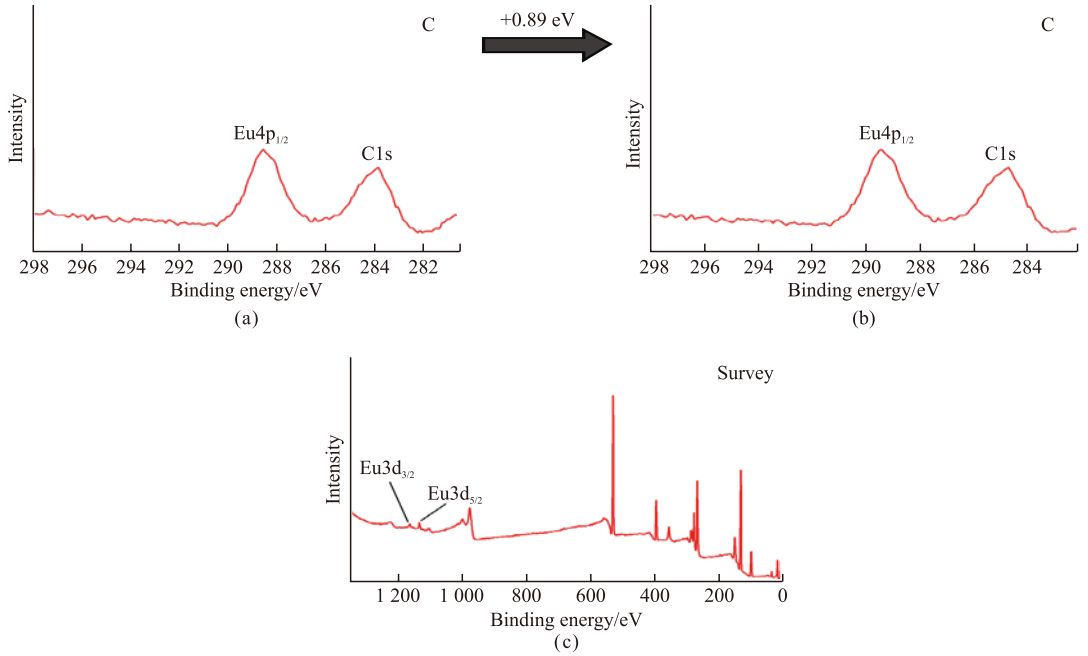


Fig.4 C1s and survey spectra of the fluorescent material ($Sr_{1-y}Eu_ySi_2O_{2-z}N_{2+2y/3}$)

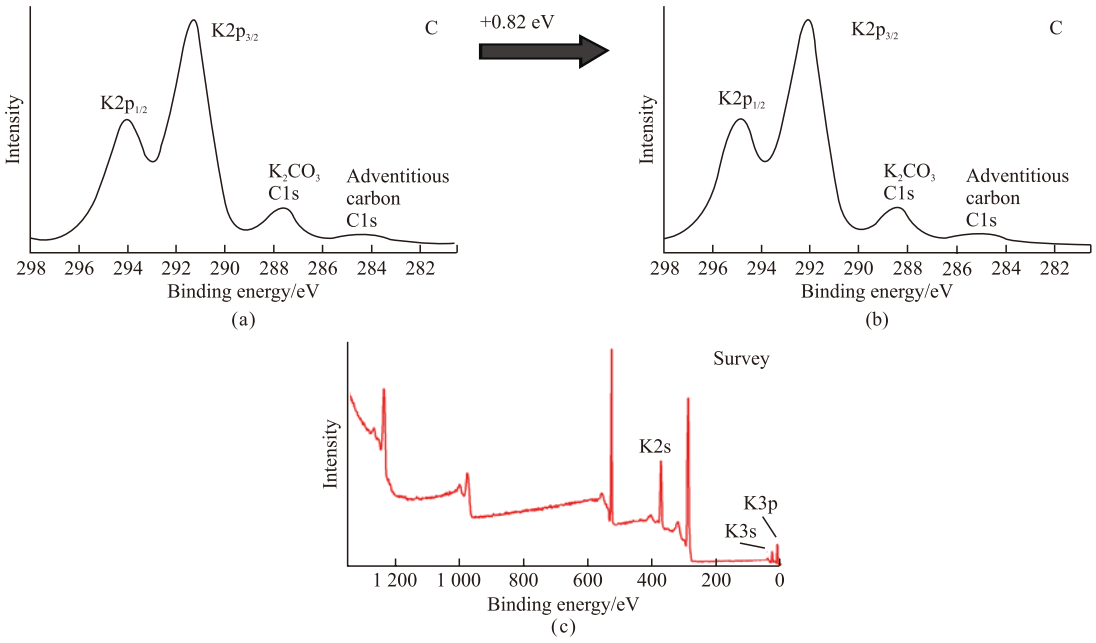


Fig.5 C1s and survey spectra of $K_2CO_3$

and $Eu3d_{5/2}$ peaks, while there is only adventitious carbon in the sample. Therefore, the peak at 283.91 eV (without calibrating) is ascribed to the adventitious carbon and the peak at 288.23 eV (without calibrating) is associated with the $Eu4p_{1/2}$. Therefore, the shift is 0.89 eV to calibrate other elements in the sample.

### 3.2 Carbon as a major part of the inorganic material on the surface

In Fig.5, there are four peaks in C1s spectrum, so these peaks should be identified before the charging effect is calibrated. According to the survey, the K element can be observed since the K3p, K3s, and K2s appear, so the peaks between 289-297 eV must be assigned to the $K2p_{1/2}$ and $K2p_{3/2}$ with the area ratio of 1:2. The peak at 283.96 eV (without calibrating) should be attributed to the C1s of the adventitious carbon, while the peak at 287.54 eV (without calibrating) can be corresponded to the C1s of the carbonate from $K_2CO_3$. Therefore, with the help of the adventitious carbon peak at 283.96 eV (without calibrating), so the shift is 0.84 eV for calibrating.

In Fig.6 the C1s spectra of TiC and $Fe_3C$ are

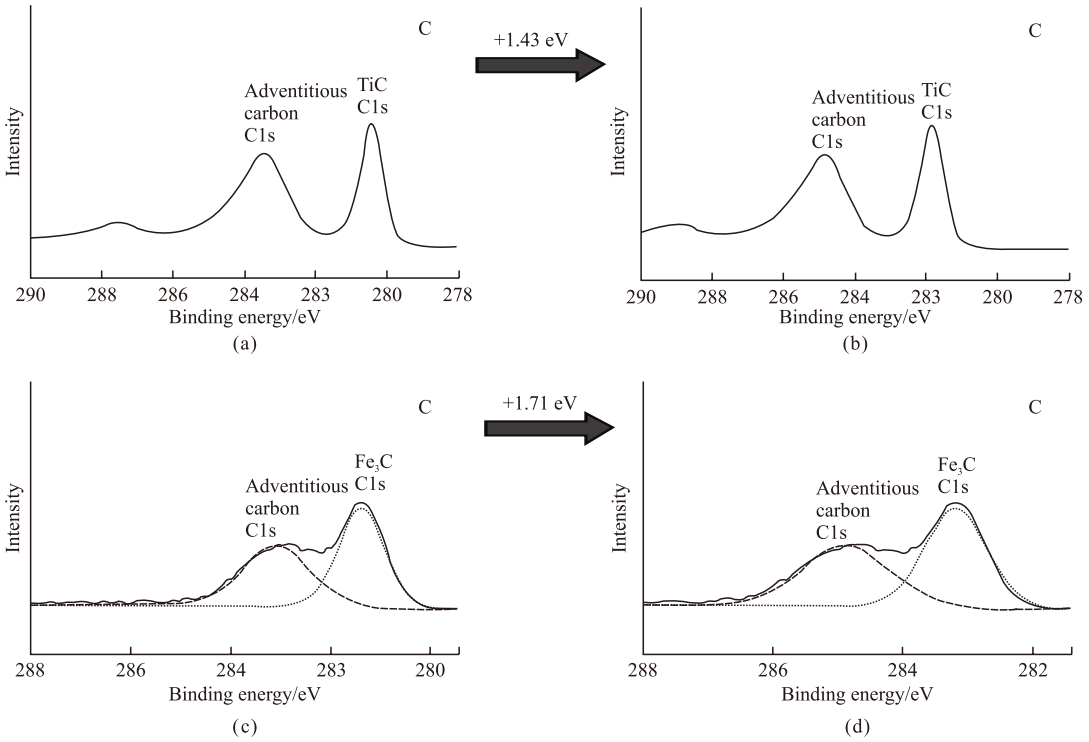


Fig.6 C1s spectra of TiC and $Fe_3C$

shown, suggesting that there are two kinds of carbons. The peak at 280.46 eV (without calibrating) is corresponded to the C1s of TiC and its FWHM is 0.75 eV, while the peak at 283.37 eV (without calibrating) is ascribed to the adventitious carbon and its FWHM is 1.47 eV in Fig.8(a). Therefore, the shift is 1.43 eV. The C1s of TiC is at 281.88 eV after using the adventitious carbon for calibrating, which is reported in the previous reports[30,31]. An obvious peak at 283.21 eV (with calibrating) in the $Fe_3C$ sample can be attributed to the C-Fe bonding[32,33]. Therefore, the analysis of the C1s spectra of TiC and $Fe_3C$ is rigorous and scientific, demonstrating the similar results with the literatures.

### 3.3 Organic carbon of the polymer materials on the surface

The surface free energy of the polymer is lower than 60 mJ/m$^2$, while that of metal and ceramic materials is more than 100 mJ/m$^2$[34,35]. For example, the surface free energies of -$CF_3$, -CClH-$CH_2$-, and -$CH_3$ are 6, 39, and 22 mJ/m$^2$, respectively. These groups with the low surface free energy have trend of surface enrichment for polymers. Therefore, there is almost no adventitious carbon on the surface of the polymers.

PE (polyethylene), PET (polyethylene terephthalate), Nylon 66, and PVDF (polyvinylidene fluoride) films are selected to study the effect of the adventitious carbon on the XPS results. Figs.7(a) and 7(b) show the C1s XPS spectra of PE films. The binding energy of the adventitious carbon and -$(CH_2)_n$- (or C-C) from PE is at the same position which is at 284.80 eV[36-38], suggesting that the shift is 1.34 eV for calibrating. Therefore, one single peak at in Fig.7(a) should be ascribed to -$(CH_2)_n$- (or C-C) due to the absence of the adventitious carbon on the surface of the polymer, which will be confirmed in the later results. The C1s peaks of PET in Figs.7(c) and 7(d) can be decomposed in four distinct peaks. Faint C1s peak with the highest binding energy is resulted from π-π* shake-up process associated with the benzene ring in the PET. C1s peak with the least binding energy is attributed to C-C (or C-H) due to the absence of the adventitious carbon on the surface of the polymer. Meanwhile, the two peaks locate in the middle, while the peak with higher binding energy is due to the contribution of ester C atoms (C=O) and the other one is due to methylene atoms bonded to one oxygen (C-O)[39-41]. Furthermore, the peak area ratio of C-C (or C-H), C-O, and C=O is 3:1:1, which is consistent with the structural features for PET. With the help of C-C (or C-H) peak in Fig.7(c), it can be found that the shift is 1.17 eV. The binding energies of C-C (or C-H), C-O and C=O are 284.80 eV, 286.38 eV, and 288.79 eV separately when the charge effect is calibrated. The C1s peaks of nylon 66 in Figs.7(e) and 7(f) can be decomposed in three distinct peaks. The component at the least binding energy is characteristic for C-C (or C-H) bond, the

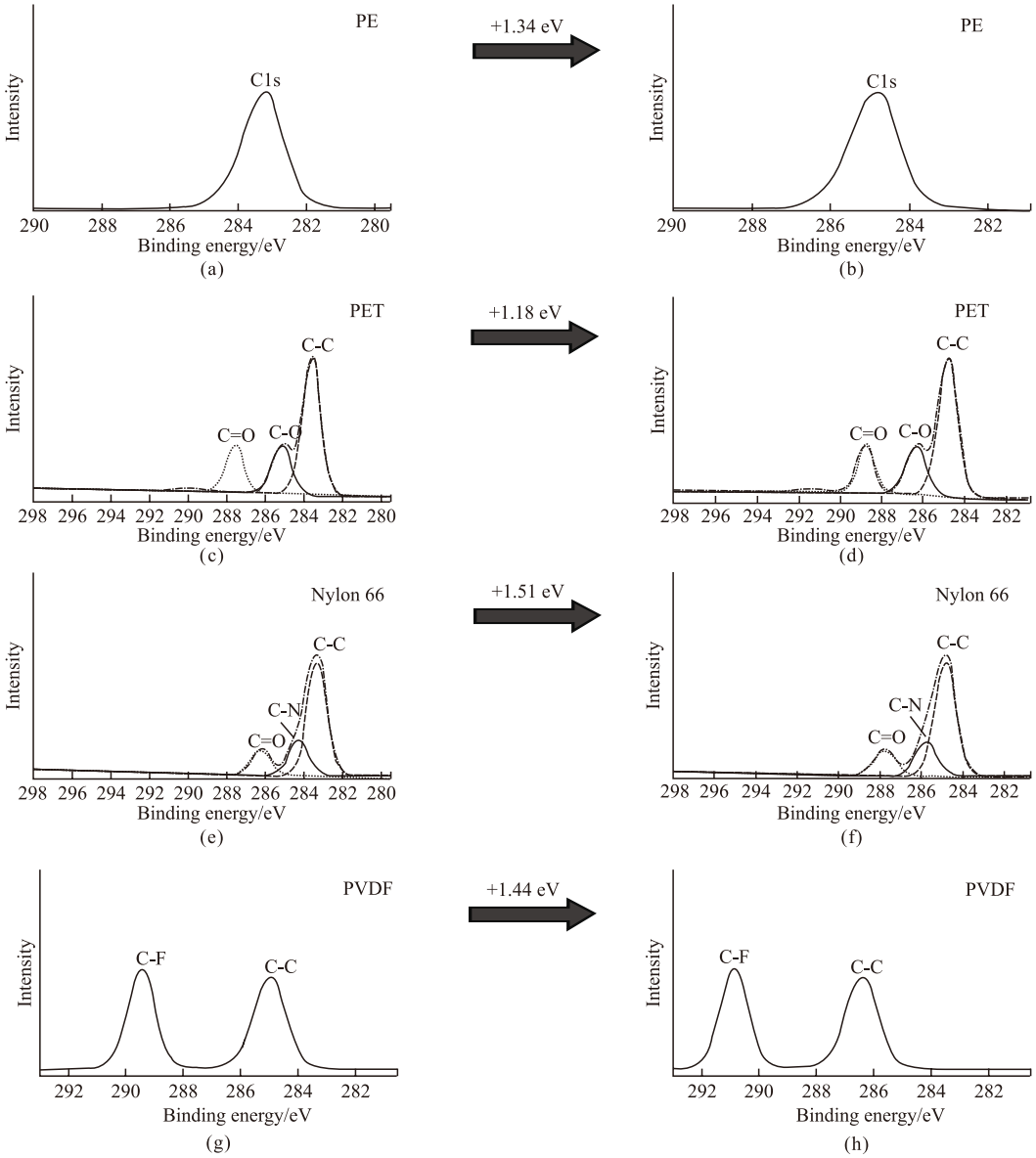


Fig.7 C1s spectra of fresh PE, PET, nylon 66, and PVDF films

component at the highest binding energy is related to the carbon atoms bonded to the -NH- group in the nylon 66, and the remaining peak is assigned to carbon atoms of amide carbonyl groups (CO-NH)[42,43]. Furthermore, the peak area ratio of C-C (or C-H), C-N and C=O is 4:1:1, which is consistent with the structural features for nylon 66. The binding energies of C-C (or C-H), C-N and C=O are 284.80 eV, 285.78 eV, and 287.81 eV separately when the shift is 1.51 eV for calibrating. There are two kinds of C1s peaks in Fig.7g and 7h. The lower binding energy is for the neutral C-C, and the other one is corresponded to the C-F in PVDF. Meanwhile, the peak areas of C-F and C-C are about equal, which is consistent with the chemical structure of PVDF[44,45]. C-C and C-F with the binding energies at 286.36 eV and 290.87 eV are obtained with the shift of 1.44 eV for calibrating, indicating that fluorine tends to induce large chemical shifts in other elements.

C1s spectra of PE, PET, nylon 66, and PVDF films that are exposed in air for different times are obtained to provide evidence for the conclusion that no adventitious carbon is on the surface of the polymers. These C1s peaks between 282 eV and 296 eV do not have undergone obvious changes, although the polymers are exposed in air for one week, two weeks, three weeks or four weeks. The intensity of C1s peak at 284.80 eV should increase markedly on condition that the adventitious carbon can be adsorbed on the surfaces of polymers. However, according to the results of Fig.8, there is no peak assigned to the adventitious carbon in PE, and the peak area ratios of all kinds of C1s are kept the same for PET, nylon 66, and PVDF.

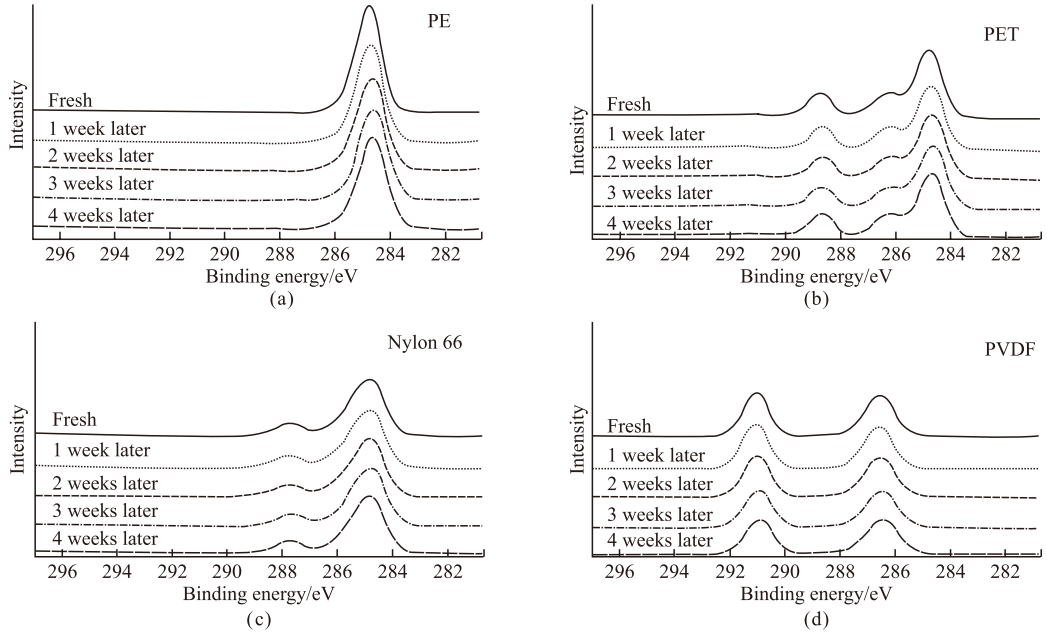


Fig.8 C1s spectra of PE, PET, nylon 66, and PVDF films exposed for different time

Therefore, it can be concluded that there is almost no adventitious carbon on the surface of the polymers, such as PE, PET, nylon 66, and PVDF.

# 4 Conclusions

It will be very hard to ensure that the sample with poor electrical conductivity is isopotential with the gold and it will take too much time to prepare the samples, when gold (paints, pens or powders) is used as the reference. Meanwhile, argon can be used as the reference when the sample is etched, so this method is usually used. However, according to several typical samples in this study, it is practical and convenient to use C1s as the reference. C1s of adventitious carbon at 284.8 eV is used as a reference for the pure $WO_3$ without containing carbon itself to calibrate the charging effect. Full dissociation should be made between the interference peaks and C1s peak, such as C1s and Ru3d peak as well as C1s and $Eu4p_{1/2}$. When carbon exits itself in the inorganic sample (such as $K_2CO_3$, TiC, and $Fe_3C$) except adventitious carbon, the carbon peaks (intrinsic and adventitious carbon) should be identified before the charging effect is calibrated. C1s spectra of the fresh polymer (PE, PET, nylon 66, and PVDF) films are calibrated with the intrinsic carbons, illustrating the reliable results in agreement with the previous researches. Furthermore, the XPS results of these polymer films exposed in air for different times indicate that no adventitious carbon is on the surface of the polymers due to the low surface free energy.

# Acknowledgements

This work is financially supported by the Fundamental Research Funds for the National Key R&D Program of China (2017YFC0210802) and Fundamental Research Funds for the Central Universities (WUT: 2019III015GX). And the tests of XPS are supported by Research and Test Center of Materials, Wuhan University of Technology.

## References

[1] Trinh QT, Bhola K, Amaniampong PN, *et al*. Synergistic Application of XPS and DFT to Investigate Metal Oxide Surface Catalysis[J]. *Journal of Physical Chemistry C*, 2018, 122: 22 397-22 406

[2] Wan Q, Liu N, Yang B, *et al*. Influence of Si Content on Properties of $Ti_{(1-x)}Si_xN$ Coatings[J]. *Journal of Wuhan University of Technology-Materials Science Edition*, 2019, 34: 774-780

[3] Paparazzo E. Some Notes on XPS Ce3d Spectra of Cerium-bearing Catalysts[J]. *Chemical Engineering Journal*, 2011, 170: 342-343

[4] Bournel F, Laffon C, Parent P, *et al*. Adsorption of Some Substituted Ethylene Molecules on Pt(111) at 95 K: NEXAFS, XPS and UPS Studies[J]. *Surface Science*, 1996, 350: 1-3

[5] Liu Q, Zhang SC, Li EM, *et al*. Facile Fabrication of $Fe_2O_3$/Nitrogen Deficient g-$C_3N_{4-x}$ Composite Catalysts with Enhanced Photocatalytic Performances[J]. *Journal of Wuhan University of Technology-Materials Science Edition*, 2019, 34: 1 018-1 023

[6] Powell CJ, Jablonski A. Surface Sensitivity of Auger-electron Spectroscopy and X-ray Photoelectron Spectroscopy[J]. *Surface and Interface Analysis*, 2011, 17: 170-176

[7] Powell CJ, Jablonski A. Surface Sensitivity of X-ray Photoelectron Spectroscopy[J]. *Nuclear Instruments and Methods in Physics Research Section A: Accelerators, Spectrometers, Detectors and Associ-*

*ated Equipment*, 2009, 601: 54-65

[8] Fouquet MW, Butcher KSA. High-sensitivity X-ray Photoelectron Spectroscopy Characterization of a Quantum Device Structure[J]. *Journal of Vacuum Science & Technology A*, 2002, 20: 2 131-2 133

[9] Wagner CD, Naumkin AV, Vass AK, *et al*. NIST Standard Reference Database 20, Version 3.4 (web version) (http://srdata.nist.gov/xps/), 2003

[10] Wagner CD, Riggs WM, Davis LE, *et al*. *Handbook of X-ray Photoelectron Spectroscopy*[M]. Perkin-Elmer Corp., Minnesota, USA, 1979

[11] Moulder JF, Stickle WF, Sobol PE, *et al*. *Handbook of X-ray Photoelectron Spectroscopy*[M]. Perkin-Elmer Corp., Minnesota, USA, 1992

[12] Zschornack G. *Handbook of X-Ray Data*[M]. Springer Corp., Berlin, Germany, 2006

[13] Tielsch BJ, Fulghum JE. Differential charging in XPS. Part I: Demonstration of Lateral Charging in a Bulk Insulator using Imaging XPS[J]. *Surface and Interface Analysis*, 1996, 24: 28-33

[14] Tielsch BJ, Fulghum JE, Surman DJ. Differential Charging in XPS. Part II: Sample Mounting and X-ray Flux Effects on Heterogeneous Samples[J]. *Surface and Interface Analysis*, 1996, 24: 459-468

[15] Tielsch BJ, Fulghum JE. Differential Charging in XPS. Part III. A Comparison of Charging in Thin Polymer Overlayers on Conducting and Non-conducting Substrates[J]. *Surface and Interface Analysis*, 1997, 25: 904-912

[16] Cazaux J. Secondary Electron Emission and Fundamentals of Charging Mechanisms in XPS[J]. *Journal of Electron Spectroscopy and Related Phenomena*, 2010, 178-179: 357-372

[17] Xu SY, Ma XX, Sun MR. Correction of Charging Effect on Structure Analyse of BCN Films by XPS[J]. *China Surface Engineering*, 2006, 1: 16-20

[18] Ding HB, Yin CS, Cai WS, *et al*. Determination of the Shift of Binding Energy of XPS by Wavelet Transform[J]. *Chinese Journal of Analysis Laboratory*, 1999, 18: 18-21

[19] Seah MP. Summary of ISO/TC 201 Standard: VII ISO 15472: 2001-surface Chemical Analysis-X-ray Photoelectron Spectrometers-calibration of Energy Scales[J]. *Surface and Interface Analysis*, 2001, 31: 721-723

[20] Watts JF, Wolstenholme J. *Applications of Electron Spectroscopy in Materials Science-An Introduction to Surface Analysis by XPS and AES*[M]. John Wiley & Sons Ltd., Chichester, UK, 2003

[21] Lesiak B, Kover L, Toth J, *et al*. C $sp^2/sp^3$ Hybridisations in Carbon Nanomaterials-XPS and (X)AES Study[J]. *Applied Surface Science*, 2018, 452: 223-231

[22] Kohiki S, Ohmure T, Kusao K. Appraisal of a New Charge Correction Method in X-ray Photoelectron Spectroscopy[J]. *Journal of Electron Spectroscopy and Related Phenomena*, 1983, 31: 85-90

[23] Lu H, Bao CL, Shen DH, *et al*. Studies of Cr/$Al_2O_3$ Interfacial Reactions[J]. *Journal of Physics and Chemistry of Solids*, 1997, 58: 257-270

[24] Brunckova H, Kanuchova M, Kolev H, *et al*. XPS Characterization of $SmNbO_4$ and $SmTaO_4$ Precursors Prepared by Sol-gel Method[J]. *Applied Surface Science*, 2019, 473: 1-5

[25] Kateryna A. Spectra Calibration in XPS[OL]. http://www.unm.edu/~kartyush/research_xps.xhtml

[26] Huang HZ, Guo QL, Gui LL. Gold-decorating Amount Correction Curve Used for Charging Shift Calibration in XPS[J]. *Chinese Journal of Analytical Chemistry*, 1986, 14: 671-676

[27] Charles DJ, Danielle G, Philippe V, *et al*. Systematic XPS Studies of Metal Oxides, Hydroxides and Peroxides[J]. *Physical Chemistry Chemical Physics*, 2000, 2: 1 319-1 324

[28] Charton P, Gengembre L, Armand P. $TeO_2$-$WO_3$ Glasses: Infrared XPS and XANES Structural Characterizations[J]. *Journal of Solid State Chemistry*, 2002, 168: 175-183

[29] Vemuri RS, Engelhard MH, Ramana CV. Correlation between Surface Chemistry, Density, and Band Gap in Nanocrystalline $WO_3$ Thin Films[J]. *ACS Applied Materials & Interfaces*, 2012, 4: 1 371-1 377

[30] Greczynsk G, Primetzhofer D, Hultman L. Reference Binding Energies of Transition Metal Carbides by Core-level X-ray Photoelectron Spectroscopy Free from $Ar^+$ Etching Artefacts[J]. *Applied Surface Science*, 2018, 436: 102-110

[31] Balazsi K. Magnetron Sputtered TiC/a:C Nanocomposite Thin Films: Deposition Parameters vs. Properties[J]. *Vacuum*, 2019, 164: 121-125

[32] Zhou JW, Zhang C, Niu TX, *et al*. Facile Synthesis of Reusable Magnetic Fe/$Fe_3C$/C Composites from Renewable Resources for Super-fast Removal of Organic Dyes: Characterization, Mechanism and Kinetics[J]. *Powder Technology*, 2019, 351: 314-324

[33] Zou MZ, Wang LL, Li JX, *et al*. Enhanced Li-ion Battery Performances of Yolk-shell $Fe_3O_4$@C Anodes with $Fe_3C$ Catalyst[J]. *Electrochimica Acta*, 2017, 233: 85-91

[34] Wang H, Gu GH, Qiu GZ. Evaluation of Surface Free Energy of Polymers by Contact Angle Goniometry[J]. *Journal of Central South University of Technology*, 2006, 37: 942-947

[35] Rojewska M, Bartkowiak A, Strzemiecka B, *et al*. Surface Properties and Surface Free Energy of Cellulosic etc Mucoadhesive Polymers[J]. *Carbohydrate Polymers*, 2017, 171: 152-162

[36] Briggs D, Fairley N. XPS of Chemically Modified Low-density Polyethylene Surfaces: Observations on Curve-fitting the C1s Spectrum[J]. *Surface and Interface Analysis*, 2002, 33: 283-290

[37] Kondyurin A, Kondyurina I, Bilek M. Radiation Damage of Polyethylene Exposed in the Stratosphere at an Altitude of 40 km[J]. *Polymer Degradation and Stability*, 2013, 98: 1 526-1 536

[38] Dorey S, Gaston F, Marque SR A, *et al*. XPS Analysis of PE and EVA Samples Irradiated at Different γ-doses[J]. *Applied Surface Science*, 2018, 427: 966-972

[39] Amor SB, Jacquet M, Fioux P, *et al*. XPS Characterisation of Plasma Treated and Zinc Oxide Coated PET[J]. *Applied Surface Science*, 2009, 255: 5 052-5 061

[40] Vesel A, Mozetic M, Zalar A. XPS Study of Oxygen Plasma Activated PET[J]. *Vacuum*, 2007, 82: 248-251

[41] Golshaei P, Guven O. Chemical Modification of PET Surface and Subsequent Graft Copolymerization with Poly(N-isopropylacrylamide)[J]. *Reactive and Functional Polymers*, 2017, 118: 26-34

[42] Bhatia QS, Burrell MC, Chera JJ. XPS Surface Studies of Injection-molded Poly(phenylene ether)/Nylon 6,6 and Poly(phenylene ether)/HIPS Blends[J]. *Journal of Applied Polymer Science*, 1992, 46: 1 915-1 925

[43] Kuzminova A, Shelemin A, Kylian O, *et al*. Study of the Effect of Atmospheric Pressure Air Dielectric Barrier Discharge on Nylon 66 Foils[J]. *Polymer Degradation and Stability*, 2014, 110: 378-388

[44] Dong L, Liu XD, Xiong ZR, *et al*. Design of UV-absorbing PVDF Membrane via Surface-initiated AGET ATRP[J]. *Applied Surface Science*, 2018, 435: 680-686

[45] Meng JQ, Chen CL, Huang LP, *et al*. Surface Modification of PVDF Membrane via AGET ATRP Directly from the Membrane Surface[J]. *Applied Surface Science*, 2011, 257: 6 282-6 290